Covid-2019 Detection Using X-Ray Images And Artificial Intelligence Hybrid Systems

COVID-2019 DETECTION USING X-RAY IMAGES AND ARTIFICIAL INTELLIGENCE HYBRID SYSTEMS

Ali Mohammad Alqudah[1,*], Shoroq Qazan[2], Hiam Alquran[1], Isam Abu Qasmieh[1]

Amin Alqudah[2]

[1] Department of Biomedical Systems and Informatics Engineering, Yarmouk University, Irbid, Jordan

[2] Department of Computer Engineering, Yarmouk University, Irbid, Jordan

[*] Corresponding Author: ali_qudah@hotmail.com
ORCID: http://orcid.org/0000-0002-5417-0043

ABSTRACT

COVID-19 leads to a severe respiratory symptom and it is associated with highly Intensive Care Unit (ICU) admissions and death. Early diagnosis with coronavirus leads to limit its wide-spreading. Real-time reverse transcription-polymerase chain reaction (RT-PCR) is the strategy that has been used by the clinician to discover the presence or absence of this type of virus. This technique has a relatively low positive rate in the early stage of this disease. Therefore, the clinicians call for another way to help in the diagnosis of COVID-2019. The appearance of x-ray chest images in case coronavirus 2019 is different from any other type of pneumonic disease. Therefore, this research is devoted to employing artificial intelligence techniques in the early detection of COVID-19 using chest X-ray images. These images are classified using deferent machine learning algorithms and their performance was tested to recognize the best of them, these algorithms include convolutional neural network (CNN), support vector machine (SVM), and Random Forest. The CNN is exploited here in two scenarios, the first one in classifying the x-ray images, and the second one in extracting the graphical features for hybrid system implantation. The extracted two features from the images for training and test parameters. According to the results of performance, the CNN performance is better than the other methods with a testing accuracy reached 95.2%.

KEYWORDS

COVID-19, Deep Learning, Machine Learning, Artificial Intelligence.

1. INTRODUCTION

The most recent type of coronavirus that is appeared in Wuhan, Hubei Province is COVID 2019. It was discovered in pneumonia cases. This type of viral pneumonia is spreading inside and outside Wuhan. This dramatically increasing in the number of infected cases around the world lead the World Health Organization named it 2019-nCoV [1]. This novel coronavirus caused severe acute respiratory syndrome is named as SARS-CoV-2 [2]. Feng Pan et al. used chest CT to assess the severity of lung involvement in COVID-19 pneumonic, they conclude that the recovering patients from COVID-19 CT-chest showed severity after 10 days after initial symptoms [3]. This new type of crown virus was discovered and identified in the viral pneumonia cases that occurred in Wuhan, which is named by the World Health Organization (WHO) as COVID-19. It is quickly spreading inside and outside of Hubei Province and even other countries, that leads to sharp increases and causing widespread panic among the people. Rabi, Firas A., et al [4] presented in their paper a summary of all current issues regarding the novel coronavirus and the disease it causes as the medical point of view.

Quadrantile and appropriate treatment for suspected cases are the most suitable methods to control the spreading of Coronavirus. The pathogenic laboratory test is used as a diagnostic tool for coronavirus suspected cases, but it consumes time with the significance of false Negative and short of supply. In the early stage detection of COVID-19, some patients may have positive pulmonary imaging manifestations, but may they have no sputum findings and they have negative test results in swabs of RT-PCR. These like cases are not diagnosed as suspected or confirmed cases [5,6].

Abdullah Ahmed [7] proposed a method for detecting coronavirus based on image processing techniques and on measuring the fringe shift concerning the background. He obtained higher contrast images using multiple-beam interference rather than just two beams interference. The refractive index of the coronavirus is concluded from a fringe shift.

Xu, Xiaowei, et al [5] employed deep learning algorithms in classification CT images for 618 subjects, into three categories, COVID -19, influenza A, and healthy persons. They obtained 86.7% accuracy among all CT cases. Wang, Shuai, et al [6] used deep learning techniques as well to extract graphical features from CT images, and supply the clinician pre-diagnosis before the pathogenic test. They achieved 89.5% accuracy and 87% sensitivity, but the accuracy of their algorithm when it is applied to the external dataset was 79.3%.

This hot topic has guided the researchers to find an accurate diagnostic tool to avoid spread it wide. All previous researches discussed this topic in a medical point of view, and the others discussed it as the appearance of CT images using deep learning, but this paper is devoted on employing machine learning algorithms in classifying and extracting graphical features of chest x-ray images automatically for COVID-19 and in Non-COVID-19 cases, and comparing between different types of classifiers to advise the most candidate one among all.

2. Materials and Methods

2.1 Dataset Description

The used dataset is the first worldwide publicly available database of COVID-19 cases with chest X-ray or CT images in addition to cases from MERS, SARS, and ARDS. All images and data are released and publicly available in this Mendeley dataset (https://github.com/ieee8023/covid-chestxray-dataset). Currently, the dataset only contains 71 chest X-ray images (48 Cases for COVID-19 and 23 for Non-COVID-19). The dataset was built by collecting images from publications as they are images that are already available [8]. This dataset has been augmented By Alqudah and Qazan using and published online and available at (https://data.mendeley.com/datasets/2fxz4px6d8/4). The augmentation has been done to prevent CNN from overfitting and memorizing the exact details of the training images. The augmentation here includes a flipping the images, rotate the image, translate the image, scale the image. The total number of images increased from 48 to 912 images which make the dataset suitable for deep learning [9]. In this work we used the original dataset proposed by Joseph Cohen with The augmentation here includes a random rotation in X-axis (-5,5) with random reflection 1, random rotation in Y-axis (-5,5) with random reflection 1 as well, random rotation (0^o-360^o), and random scaling (0.5-1). Figure 1.a shows an x-ray image for the non-COVID-19 subject, and Figure 1.b represents the subject with COVID-19.not the augmented one by Alqudah and Qazan. Figure 1.a shows an x-ray image for the non-COVID-19 subject, and Figure 1.b represents the subject with COVID-19.

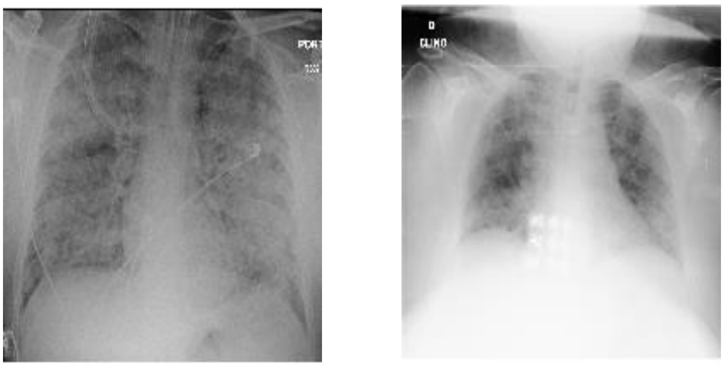

(A) (B)

Figure 1. Sample Images for Used Dataset; (A) Non-COVID-19; (B) COVID-19 Subject [8].

2.2 Convolutional Neural Network

Convolution Neural Networks (CNNs) is a type of traditional artificial neural network (ANN), which is composed of neurons that own learnable weights alongside biases. An input image pixel is entered for every neuron, followed by the calculation of a dot product and the elective non-linearity capture. [10]. The input layer represents an image with enhancement such as mean subtraction and feature-scaling. The most distinguished feature of CNN's over ANNs is the huge number of hidden layers, which consist of convolution layers that are convolved the image with learnable filters, and each one results in the feature map in the output image.

The spatial coordinate of the feature map is reduced by pooling layers. This is performed by applying a window on the image with a specific stride of every step and voting the maximum value of the pixel and putting it in the new image. There is another method can be applied in the pooling layer based on the average value. ReLU layer which introduces the nonlinearity for the network its function is $f(x) = \max(0, x)$ [10]. The last layer is a fully connected layer which represents the output layer that has the classification value which is serving the classification result as a single vector of probabilities [11].

The AOCT-NET [12] is employed in this paper to classifying the chest x-ray images. It is started by the first convolutional layer which uses 32 filters with size 3×3 and one padding zeros, whereas the rest convolutional layers devoted 16 filters with the same size, except the third one that it is used 8 filters only. For time-consuming, accelerating training stage purposes, and decreasing the sensitivity of the network initialization, the batch normalization layer is added between the convolutional layer and the nonlinearity layer (RELU). Max pooling layer is utilized in AOCT-NET with window size 2×2 and increments 2 pixels as well. The output layer consists of a fully connected layer with an output size 2, a softmax layer, and a classification layer. Figure 2 illustrates the graphical representation of AOCT-NET.

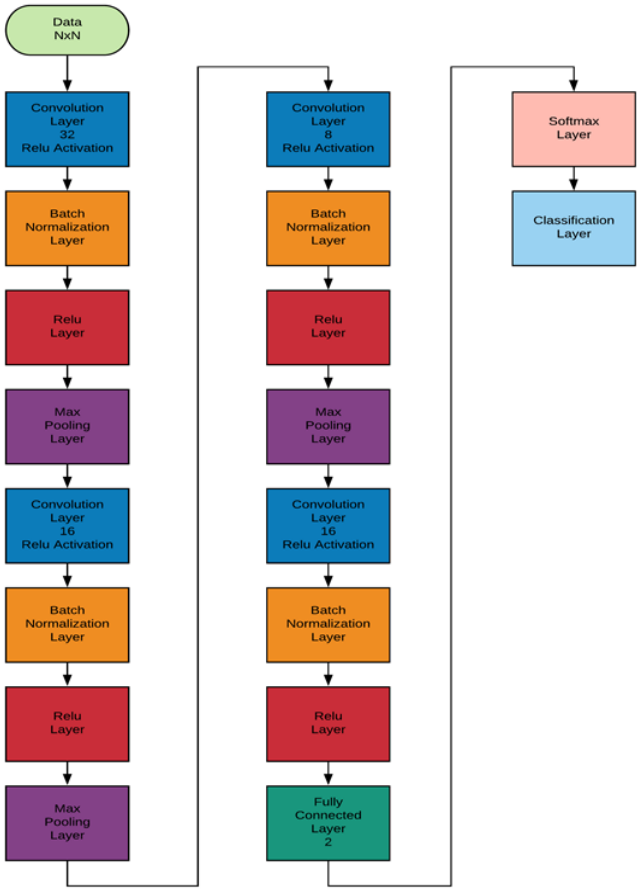

Figure 2. AOCT-NET graphical representation.

2.3 Features Extraction

The automated graphical features are extracted from the fully connected layer of AOCT-NET. One feature is distinguished from the COVID-19 cases and the other for non-COVID-19. The scatter distribution for both two features is represented in Figure 3 where the blue dots indicate to COVID-19 feature, while the red points represent the non-COVID-19 descriptor as well. The time required for extracting the features from the fully connected layer in the training stage for the whole dataset is 2.26 seconds.

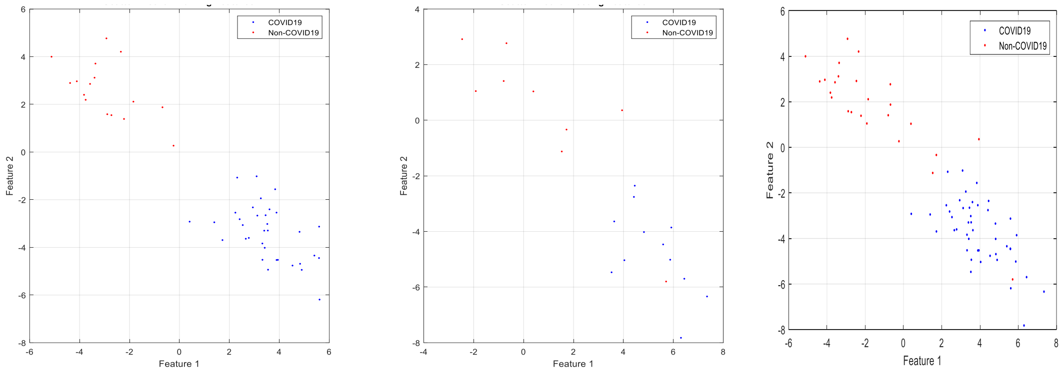

(A) (B) (C)

Figure 3. the scatter distribution of two distinguished extracted features (A) from Training Set; (B) from Testing Set; (C) All Extracted Features from both sets.

These features are used to build models using Support Vector Machine (SVM) and Random Forest (RF) classifiers.

2.4 Support Vector Machine Classifier

Linear SVM is the simplest form among all SVM types, and it is used when the data is separated linearly, but if the number of features is more than two then the data can be separated using hyperplane, the corresponding equation describes the linear form

$$f(x) = \boldsymbol{w^T}.x + b$$

The above equation is minimized using cost function which is expressed by the following equation

$$j(w) = \frac{1}{2}\boldsymbol{w^T w} \ = \boldsymbol{\frac{1}{2}|w|^2}$$

Various types of hyperplanes can be separated from the data. Therefore, the optimal solution is determined by the degree of strictness in user-specified constraints. The constraint level can be specified to control the margins between the two discriminated classes. This can be obtained using Lagrangian multipliers. Constrains parameters are δ which handles the misclassification degree and c which is the regularization parameter. The function is expressed in equations below:

$$J(w, \delta) = \frac{1}{2}\|w\|^2 + C\sum_{i=1}^{l} \delta_i^2 \text{ Such that } \quad y_i(w^T x_i + b \geq 1 - \delta_i \ \delta_i > 0, i = 1,2, \ldots \ldots .., l$$

If the data cannot be separated linearly, then another technique can be applied by mapping the input features into higher dimensional features to determine the separating hyperplane. This type of mapping function is called the kernel. There are different types of kernels, quadratic, polynomial and radial basis functions. The kernel that has been employed in this paper is Gaussian radial basis function (RBF), which is given by the following equation with $\sigma > 0$ which defines the kernel width [13].

$$K(x, y) = \exp\left(-\frac{\|x - y\|}{2\sigma^2}\right)$$

2.5 Random Forest Classifier

The Random Forest algorithm was established by Breiman in 2001. It is consists of a large number of individual decision trees that work as a collaborative. Each distinct tree in this classifier type spits out a class prediction and the class with the most elections to be our model's prediction. The vital impression behind the random forest is the simplicity and the powerful. In data science-speak, the reason that is due to the random forest model works so well is many relatively uncorrelated models [12].

2.6 Performance Evaluation

The confusion matrix is the most commonly used method to evaluate the performance of the artificial algorithm that has been used. It compares the output of the system with the reference data. The confusion matrix indicates the most common metrics, such as accuracy, specificity, sensitivity, and precision. To evaluate each one, the four statistical indices that have been used; true positive (TP), false positive (FP), false negative (FN) and true negative (TN) were calculated, and consequently, the Accuracy, Sensitivity, Precision, and specificity were computed as follows:

$$Accuracy = \frac{\mathrm{TP+TN}}{\mathrm{TP+FP+TN+FN}} \tag{1}$$

$$\mathrm{Sensitivity} = \frac{\mathrm{TP}}{\mathrm{TP+FN}} \tag{2}$$

$$\mathrm{Precisions} = \frac{\mathrm{TP}}{\mathrm{TP+FP}} \tag{3}$$

$$\mathrm{Specificity} = \frac{\mathrm{TN}}{T\mathrm{N+FP}} \tag{4}$$

The accuracy is indicated about the ability of the classier to differentiate between the classes correctly, while sensitivity refers to its ability to correctly detect the true positive, specificity evaluates the actual negatives that are correctly identified by the classifier, and precision indicates to its ability to predict positive from how many of them are positive [14]. A receiver operating characteristic curve (ROC) is a graphical that representation the classifier model performance. It has two parameters, true positive rate (TPR) and false-positive rate (FPR), each parameter is computed as following [15]:

$$TRP = \frac{TP}{TP+FN} \tag{5}$$

$$FPR = \frac{FP}{FP+TN} \tag{6}$$

It shows TPR versus FPR at various classification thresholds. For the lower one, the classifier can discriminate more subjects, which causes increases in both False Positives and True Positives [16].

3. RESULTS

The proposed methodology, using the CNN-based system for classification of chest X-ray images was successful in classifying the grayscale images with high performance. CNN has been used to show 95.2% accuracy, but the hybrid system, which is extracted the features from the fully connected layer in the CNN obtained 90.5 in SVM classifier and 81% using RF classifier as well. The training and testing confusion matrices for all classifiers that have been employed are shown in Figure. 4 A, B, C, D, E, and F. While Table 1 shows a comparison between all performance evaluations values for the used classifiers in the training stage and the Table 2 represents the performance evaluation for the test stage for all classifiers that have been used. Table 3 is exploited to the computation time for each system individually.

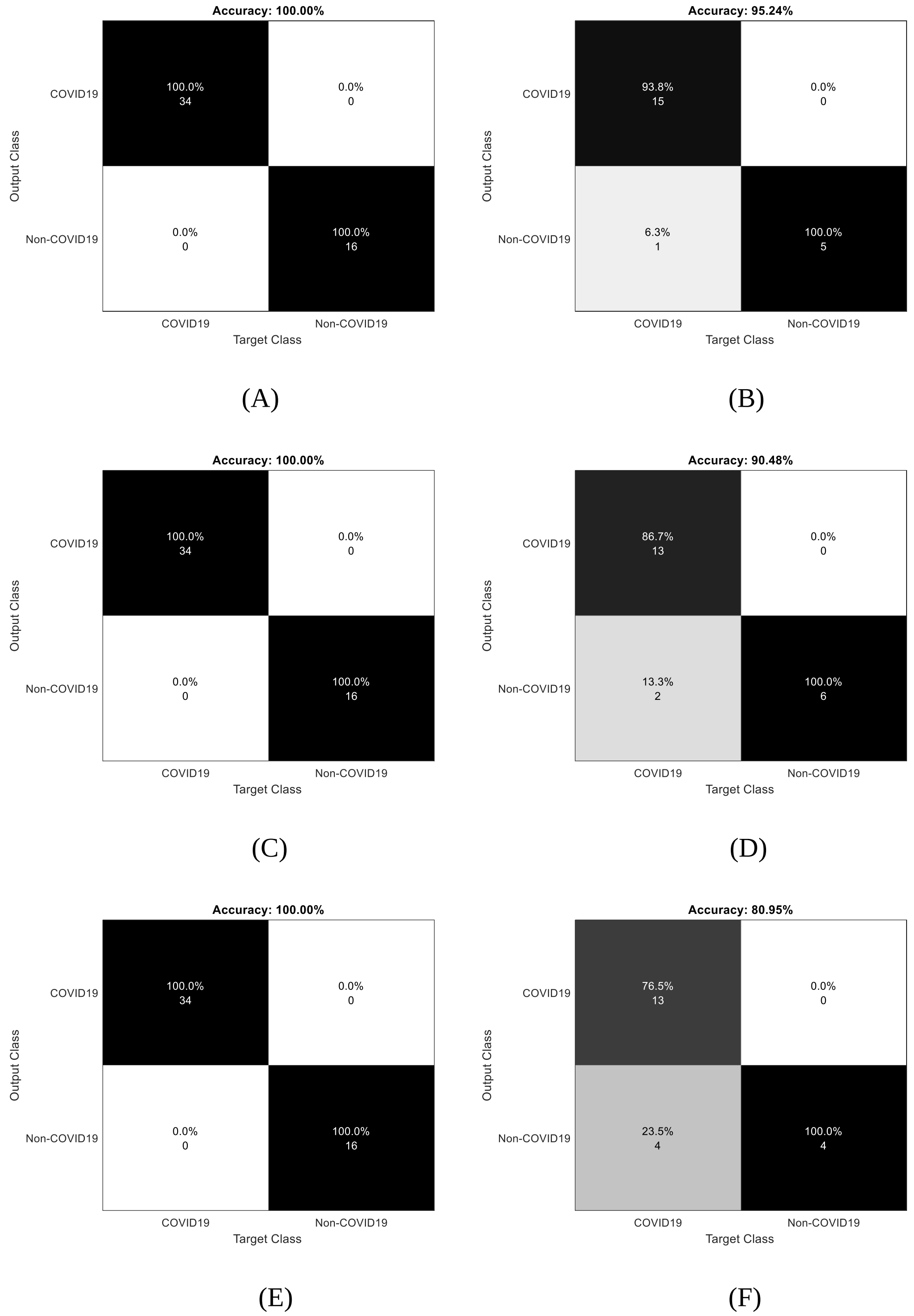

Figure 4. Testing Confusion Matrices; (A): CNN-Softmax Training, (B): CNN-Softmax Test, (C): CNN-SVM Training, (D): CNN-SVM Test (E): CNN-RF Training, (F): CNN-RF Test.

Table 1. Training Performance Evaluation of Classifiers

Classifiers	**Performance Evaluation Metric**			
	Accuracy %	**Sensitivity %**	**Specificity %**	**Precision%**
CNN-Softmax	100	100	100	100
CNN-SVM	100	100	100	100
CNN-RF	100	100	100	100

TABLE 2. Testing Performance Evaluation of Classifiers

Classifiers	Performance Evaluation Metric			
	Accuracy%	**Sensitivity %**	**Specificity %**	**Precision %**
CNN-Softmax	95.2	93.3	100	100
CNN-SVM	90.5	86.7	100	100
CNN-RF	81	76.5	100	100

TABLE 3. Testing Performance Evaluation of Classifiers.

Classifiers	Time (s)
AOCT-NET	0.299704
SVM	0.168938
Random Forest	0.551982

Figure. 5 shows the classification error development during building random forest classifiers while Fig. 6 shows the built model.

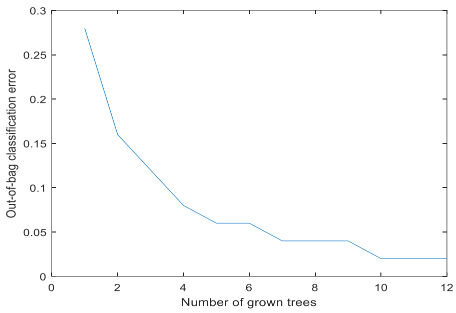

Figure 5.The Error Variation Over Number of Used Trees.

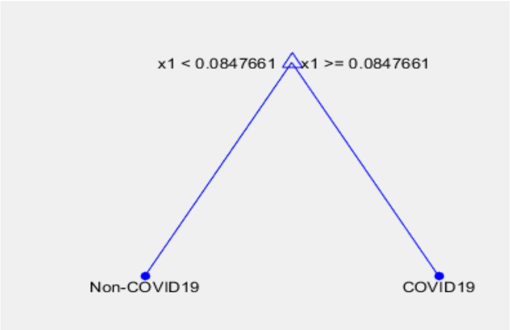

Figure 6. The Built Random Forest Model for Classification

4. DISCUSSION

The proposed methodology was applied on Chest X-ray images dataset, where CNN is utilized in two scenarios, the first one is in classification to COVID-19 and non-COVID-19, in the second scenario it is employed to extract graphical features for hybrid system implementation. These two features were extracted from the fully connected layer from each image. CNN was trained using Adaptive Moment Learning Rate (ADAM) solver after applying data augmentation to increase the number of the dataset and to avoid overfitting during the training stage of the CNN. Then, these features are fed into two types of classifiers; SVM and RF. The performance of all classifiers in the training stage was 100%, but in the test stage, deep learning classification using the CNN classifier is performed better than the hybrid systems. For the hybrid system, the SVM obtained better results than RF that is due RBF method, but RF performance was the lowest among all. That it is because built trees that combined with majority voting technique for each input vector which is two, in addition to that RF is constructed by using different base learners, and for each base learner an independent binary tree adopting recursive partitioning has been built.

5. CONCLUSION

In this paper, we utilized the benefits of using artificial intelligence techniques including deep learning (CNN using softmax classifier) and machine learning (SVM and RF) in building a system that can discriminate between COVID-19 and non-COVID-19 X-ray images. As shown in Table 3 the time consuming is less in softmax classifier than other systems (hybrid systems). The results can be improved when we can obtain a huge dataset of chest X-ray images in addition to if we build a model that used CT images. On the other hand, in the future, we can use various types of classifiers that may be applied besides different types of features that could be extracted such as local binary pattern (LBP), texture features, etc. which are used to describe the texture of the chest.

COMPLIANCE WITH ETHICAL STANDARDS

Conflict of interest The authors declare no conflict of interest.

Ethical approval This article does not contain any studies with human participants or animals

performed by any of the authors.

Funding No funding received for this research.

REFERENCES

[1] Stoecklin, Sibylle Bernard, et al. "First cases of coronavirus disease 2019 (COVID-19) in France: surveillance, investigations and control measures, January 2020." Eurosurveillance 25.6 (2020).

[2] Jin, Ying-Hui, et al. "A rapid advice guideline for the diagnosis and treatment of 2019 novel coronavirus (2019-nCoV) infected pneumonia (standard version)." Military Medical Research 7.1 (2020): 4.

[3] Pan, Feng, et al. "Time course of lung changes on chest CT during recovery from 2019 novel coronavirus (COVID-19) pneumonia." Radiology (2020): 200370.

[4] Rabi, Firas A., et al. "SARS-CoV-2 and Coronavirus Disease 2019: What We Know So Far." Pathogens 9.3 (2020): 231.

[5] Xu, Xiaowei, et al. "Deep Learning System to Screen Coronavirus Disease 2019 Pneumonia." arXiv preprint arXiv:2002.09334 (2020).

[6] Wang, Shuai, et al. "A deep learning algorithm using CT images to screen for Corona Virus Disease (COVID-19)." medRxiv (2020).

[7] Hamed, Abdallah Mohamed. "Image processing of corona virus using interferometry." Optics and Photonics Journal 6.05 (2016): 75.

[8] Joseph Paul Cohen, COVID-19 image data collection, https://github.com/ieee8023/covid-13

[9] Alqudah, Ali Mohammad; Qazan, Shoroq (2020), "Augmented COVID-19 X-ray Images Dataset", Mendeley Data, v4http://dx.doi.org/10.17632/2fxz4px6d8.4

[10] Żejmo, Michał, et al. "Classification of breast cancer cytological specimen using convolutional neural network." Journal of Physics: Conference Series. Vol. 783. No. 1. IOP Publishing, 2017.

[11] Spanhol, Fabio Alexandre, et al. "Breast cancer histopathological image classification using convolutional neural networks." 2016 international joint conference on neural networks (IJCNN). IEEE, 2016.

[12] Alqudah, Ali Mohammad. "AOCT-NET: a convolutional network automated classification of multiclass retinal diseases using spectral-domain optical coherence tomography images." Medical & biological engineering & computing 58.1 (2020): 41-53.

[13] Hiam Hamad. 3D modeling and Al-Quran classification of microcalcification patterns in breast computed tomography. Diss. UNIVERSITY OF MASSACHUSETTS LOWELL, 2014.

[14] Alqudah AM, Alquraan H, Abu-Qasmieh I, Al-Badarneh A. Employing Image Processing Techniques and Artificial Intelligence for Automated Eye Diagnosis Using Digital Eye Fundus Images. In Journal of

Biomimetics, Biomaterials and Biomedical Engineering 2018 (Vol. 39, pp. 40-56). Trans Tech Publications.

[15] Alqudah, Ali Mohammad. "Towards classifying non-segmented heart sound records using instantaneous frequency based features." Journal of medical engineering & technology 43.7 (2019): 418-430.

[16] Hand, David J., and Robert J. Till. "A simple generalisation of the area under the ROC curve for multiple class classification problems." Machine learning 45.2 (2001): 171-186.